LOADING RATE EFFECTS DUE TO VISCOUS PROPERTY ON THE STRENGTH AND DEFORMATION PROPERTY OF GEOSYNTHETIC REINFORCEMENT

W. Kongkitkul
University of Tokyo

D. Hirakawa
Tokyo University of Science

T. Uchimura
University of Tokyo

F. Tatsuoka
[illegible]

ABSTRACT: In the current design methodology, the long-term design tensile strength of a given geosynthetic reinforcement is obtained by reducing with a relatively large creep reduction factor the strength from tensile tests at a relatively high strain rate. This method could mislead to a wrong notion that creep is a degrading phenomenon. The method is linked to the isochronous concept, which states that the present tensile load is a unique function of instantaneous strain and elapsed time since the start of loading. A series of tensile tests on a PET geocomposite were performed. Based on the test results, the following is shown: 1) the rupture strength is a unique function of strain rate at rupture, independent of pre-rupture loading history; 2) creep deformation takes place due to material viscous properties and therefore is not a degrading phenomenon, and the isochronous concept is not relevant; and 3) a non-linear three-component model taking into account the viscous properties in addition to elasticity and strain-irreversibility while not introducing any negative effects of time elapsing on the model parameters can simulate the whole observed load-deformation characteristics during monotonic loading at strain rates, different up to factor of 100, and at step changes in the strain rate and during creep and stress relaxation tests applied during otherwise primary loading and global unloading.

1 INTRODUCTION

To use on-site high-water content soil as the backfill for a geosynthetic-reinforced soil (GRS) structure, the reinforcement should have functions of both tensile-reinforcing and drainage. Several different types of geocomposite consisting of a woven geotextile or a yarn for tensile-reinforcing and a non-woven geotextile for drainage are often used. The long-term drainage function of a given geocomposite, in particular whether it is clogged with fines particles from the backfill, is firstly ensured. The long-term design rupture strength of a geocomposite is usually obtained in the same way as other types of tensile reinforcement such as polymer geogrids. That is, the long-term design tensile strength is obtained by reducing with a relatively large creep reduction factor the rupture strength obtained from tensile tests performed at a relatively high strain rate. However, this design methodology could mislead to a wrong notion that creep is a degrading phenomenon. On the other hand, with a number of different types of geosynthetic reinforcements including polymer geogrids, pre-rupture creep deformation does not affect the tensile ruptured strength (e.g., Voskamp et al. 2001; Hirakawa et al. 2002 & 2003; Kongkitkul et al. 2002 & 2003). Rather, the rupture strength is a function of strain rate at rupture.

The current design methodology is linked to the isochronous concept, which states that the present tensile load is a unique function of instantaneous strain and elapsed time since the start of loading. Hirakawa et al., (2002, 2003) and Kongkitkul et al. (2002, 2003) showed that the isochronous concept is not able to predict the load-strain behaviour of a given geosynthetic reinforcement for general arbitrary loading histories, in particular the one observed after the loading is restarted at a constant strain rate following creep loading.

In the present study, the load-strain-time behaviour of one type of geocomposite was thoroughly evaluated by performing a series of continuous monotonic loading tests (ML) at different constant strain rates as well as unconventional tests in which the strain rate was changed stepwise and creep and stress relaxation loading tests were perfor-

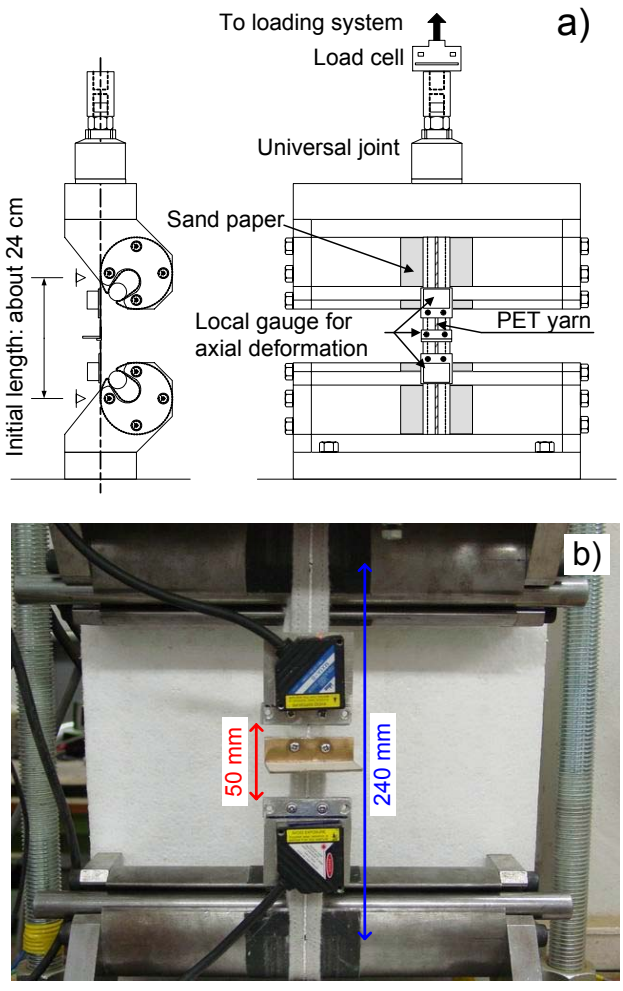

Figure 1. Tensile loading apparatus with a test specimen.

med during otherwise ML. The test results were successfully simulated by the three-component model that has been developed for geomaterials (Di Benedetto et al., 2002; Tatsuoka et al., 2002).

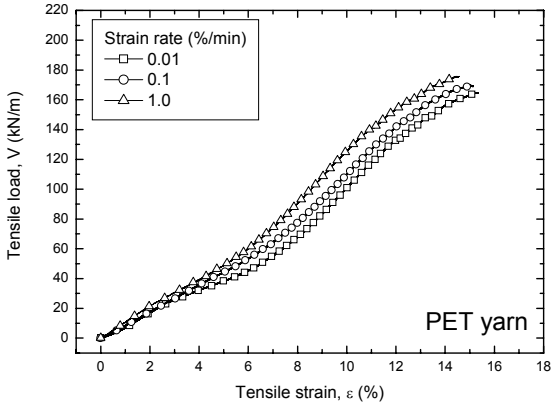

Figure 2. $V-\varepsilon$ relations from ML tests at different strain rates.

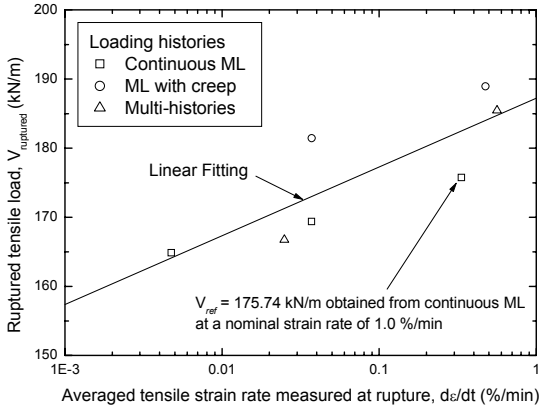

Figure 3. Rupture strength as a function of strain rate.

2 TEST APPARATUS AND PROCEDURE

A strain-controlled tensile loading apparatus having a capacity of 50 kN was used. It consists of a precise gear system with practically no backlash upon load reversal. By using this loading system, it is possible: a) to smoothly switch the loading mode between displacement and load control phases and between creep or relaxation stage and constant strain rate loading/unloading phases; b) to change the strain rate stepwise or gradually by a factor up to 3,000; and c) to apply small-amplitude cyclic loading to evaluate the equivalent elastic property at any arbitrary moment.

The gripping device consists of a pair of roller-clamps, each consisting of a steel cylinder having a smooth surface with a groove made to grip a specimen with a small steel rod (**Fig. 1a**). A sheet of sand paper was firmly glued on the surface of the clamp where a specimen was wrapped around to prevent any slippage during a test.

3 TEST MATERIAL

PET yarn retrieved from the "Polyfelt ROCK PEC 150" geocomposite, provided by Polyfelt GmbH, was used. The geocomposite consists of a planar needle-punched non-woven geotextile made of continuous polypropylene (PP) filament for drainage and high-strength polyester (PET) yarns in the longitudinal direction for tensile-reinforcing. The spacing between two parallel yarns is about 5 mm. The tensile strength of the non-woven geotextile sheet is negligible when compared with the one of the PET yarns.

In tests using a geocomposite specimen consisting of more than one yarn cut to have the initial length of 900 mm, significant necking took place due to the so-called Poisson's effects with the non-woven geotextile portion. This necking phenomenon does not take place when placed in the proto-type backfill while it may affect the measured tensile load-strain characteristics. On the other hand, tests on a single extracted PET yarn were not successful either because a pair of laser displacement transducers could not be properly fixed to the single yarn. As the final solution, the specimens consisting of three yarns with a non-woven geotextile with a width of about 15 mm were prepared by cutting the original geocomposite in the longitudinal direction and subsequently the two side yarns were removed (**Fig. 1b**). These specimens will hereinafter be called "PET yarn specimens". Each specimen has a total initial length of 900 mm, an unconfined initial length of 240 mm (excluding those wrapped around the clamps) and an initial gauge length of 50 mm, over which tensile strains were measured locally by using a pair of laser displacement transducers.

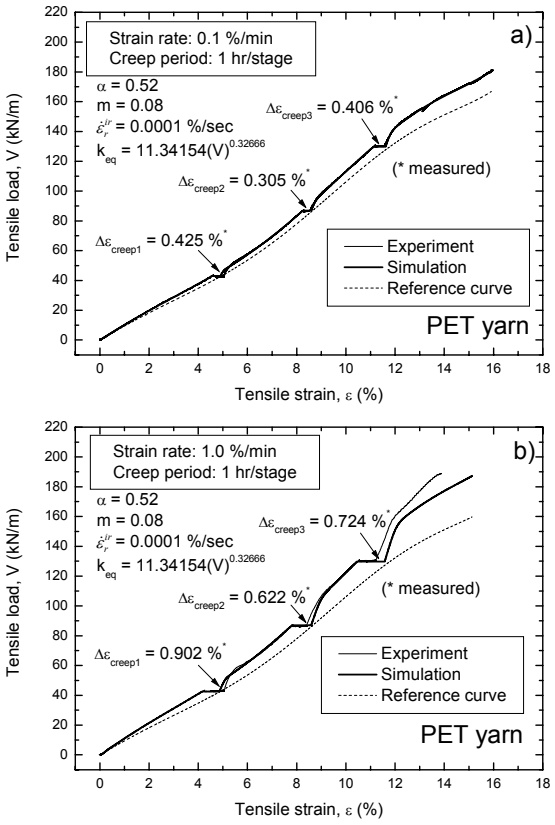

Figure 4a&4b. $V-\varepsilon$ relations from ML tests with creep tests with two different initial strain rates and their simulation.

4 TEST RESULTS AND DISCUSSION

Fig. 2 shows the relationships between the tensile load, V, and the tensile strain, ε, obtained from continuous ML tests at constant strain rates of 0.01; 0.1 and 1.0 %/min. **Fig. 3** summarises the ruptured strengths from these tests and those with more complicated loading histories (shown

below), plotted against the logarithm of the strain rate at rupture. The ruptured strength from a continuous ML test at a strain rate of 1.0 %/min, equal to 175.74 kN/m ($Vref$) as shown in **Fig. 3**, was used as the reference strength for creep load levels. **Figs. 4a** & **4b** shows the results from continuous ML tests with creep loading tests at three different load levels, equal to 25 %, 50 % and 75 % of $Vref$, during otherwise ML at strain rates of 0.1 and 1.0 %/min. Each creep loading test lasted for one hour. The results from model simulation will be explained later. The following trends of behaviour can be clearly seen from these figures:

1) The effects of strain rate on the pre-peak $V-\varepsilon$ relations and the ruptured strength are significant. That is, a) $V-\varepsilon$ relations at faster strain rates are stiffer; and b) the ruptured strength increases proportionally to the logarithm of the strain rate at rupture.
2) The creep strain that develops for a given period of creep loading at a given load level increases with an increase in the initial strain rate at the start of creep loading, showing the importance of control of the initial creep strain rate in the evaluation of creep strain. Creep deformation of a given prototype GRS structure would be overestimated if it is predicted without taking this factor into account while based on results from conventional laboratory creep tests in which the initial creep strain rate is much higher than the one with the prototype structure.
3) For a given period of creep loading with a given initial strain rate, the creep strain first decreases then increases with an increase in the creep load level. This peculiar behaviour is due to the *S*-shaped $V-\varepsilon$ relations as shown in **Fig. 2**: that is, the tangent stiffness increases as the load increases from 25 % to 50 % of $Vref$ while it decreases as the load increases from 50

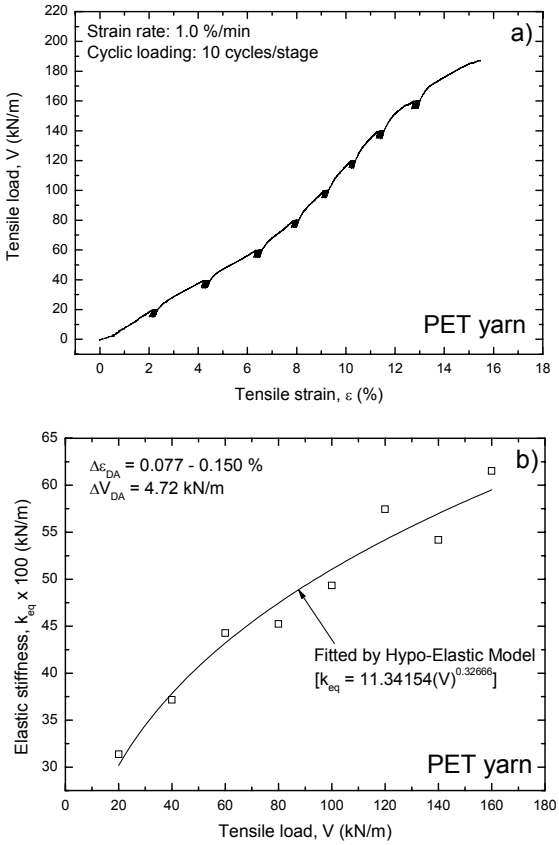

Figure 6a&6b. Evaluation of elastic properties.

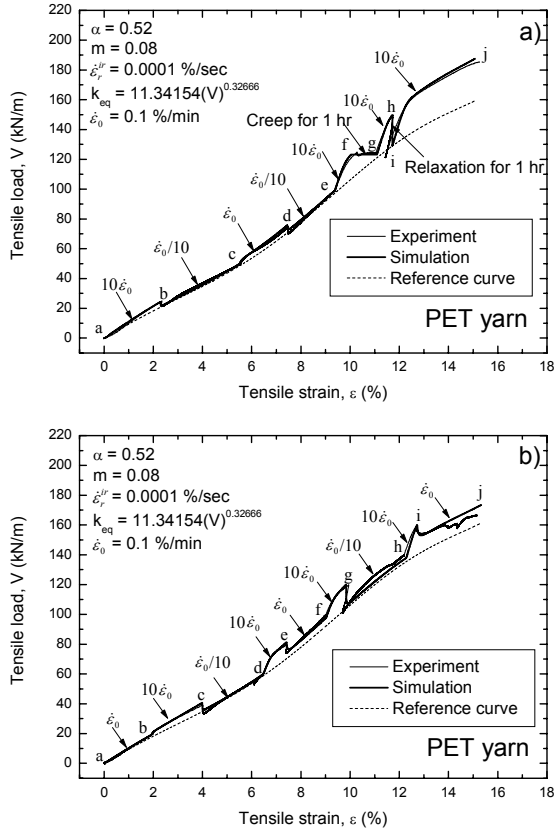

Figure 5a&5b. $V-\varepsilon$ relations from ML tests with different sequences of step changes in the strain rate, creep and stress relaxation tests; and their simulation.

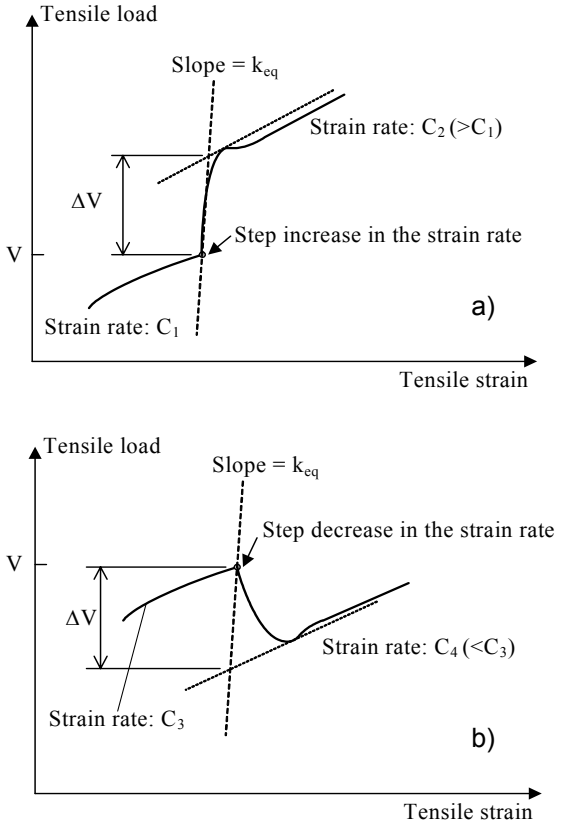

Figure 7a&7b. Definitions of load jump upon a step change in the strain rate.

% to 75 % of $Vref$. The three-component model can simulate this peculiar creep behaviour as shown later in this paper.

4) When ML is restarted following each creep loading test, the $V-\varepsilon$ relation exhibits a very high tangent stiffness compared with the one observed at the same load level during continuous ML without any intermission of creep. Then, the $V-\varepsilon$ curve tends to rejoin the curve observed during continuous ML, without showing any effects of previous creep loading history on the subsequent load-strain characteristic at higher load levels. This fact indicates that creep loading has no deteriorating effects on the strength and deformation characteristics but it is a viscous response of the test material.

To better understand the viscous effects on the $V-\varepsilon$ behaviour, other two tests with multiple loading histories including stepwise changes in the strain rate, creep and stress relaxation tests were performed, **Figs. 5a** & **5b**. For confirmation, the sequences of changes in the strain rate were made opposite in the two tests. It may be seen that the tensile load exhibits a significant sudden increase/decrease upon a stepwise increase/decrease in the strain rate.

To obtain irreversible strains from measured total strains, the equivalent elastic stiffness keq was evaluated by performing small-amplitude cyclic loading tests (10 cycles/stage) at different load levels during otherwise ML at a constant strain rate of 1.0 %/min (**Fig. 6a**). **Fig. 6b** shows the relationship between the value of keq (the average for 10 cycles of the linearly fitted slope of reloading $V-\varepsilon$ curve) and V . It may be seen that the value of keq is not constant but increases with V following the non-linear relation shown in Fig. 6b. Then, the irreversible strain increment $\dot{\varepsilon}^{ir}$ was obtained as: $d\varepsilon^{ir}=d\varepsilon-d\varepsilon^{e}$, where $d\varepsilon^{e}$ is the elastic strain increment obtained as: $d\varepsilon^{e}=dV/keq(V)$; dV is a given load increment. According to the three-component model (explained later), the loading rate effects due to viscous property are controlled basically by the irreversible strain rate, $\dot{\varepsilon}^{ir}=d\varepsilon^{ir}/dt$.

The amount of load jump per unit width, ΔV upon each step change in $\dot{\varepsilon}^{ir}$, as defined in **Figs. 7a** & **7b**, was obtained from the test results presented in Fig. 5. **Fig. 8a** shows the relationships between ΔV and the instantaneous load V for different changing ratios of $\dot{\varepsilon}^{ir}$. It may be seen that ΔV is always proportional to V for the respective ratio of $\dot{\varepsilon}^{ir}$. Based on this fact, each ratio $\Delta V/V$ was plotted against the logarithm of the ratio of the values of $\dot{\varepsilon}^{ir}$ after and before a stepwise change (**Fig. 8b**). It may be seen that the relation is unique and linear. The slope β of relation, equal to 0.080, is the parameter representing the viscous properties and will later be linked to the model parameters. **Table 1** shows the β values of other types of polymer geosynthetic reinforcements (Hirakawa et al. 2003). The β value of the geocomposite is within a very small range (between 0.0665 and 0.1428) of the other types of geosynthetic reinforcement that have been evaluated by the authors.

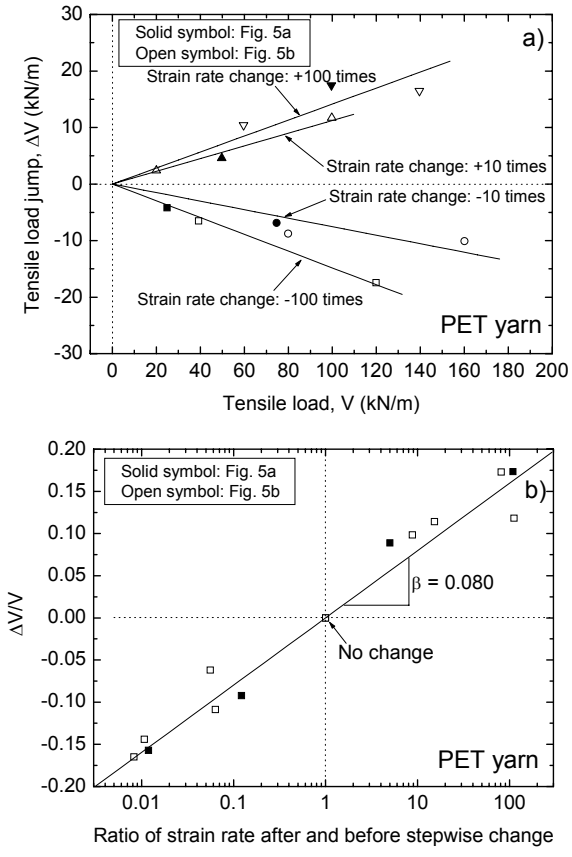

Figure 8a&8b. a) ΔV and V relation; and b) $\Delta V/V$ and log. of strain rate ratios.

Table 1. β - values obtained from different geogrids (after Hirakawa et al., 2003)

Fibre material	Specimen condition	Ruptured strength (kN/m)*	β - value
Polyester	Virgin	39.2	0.1428
Polyarylate	Virgin	88.0	0.0732
Polyvinyl alcohol	Virgin	60.8	0.1319
Aramid	Virgin	56.0	0.0665
HDPE	Virgin	50.0	0.1132
Polyvinyl alcohol	Aged (8 yrs)	59.0	0.1595

* at a strain rate = 1.0 %/min

It may be seen from the above that the viscous properties observed with geosynthetic reinforcements, including the geocomposite tested in this study, are highly non-linear, unlike the Newtonian type viscosity, for which $V=\eta\cdot\Delta\varepsilon^{ir}$ (η = constant) is relevant.

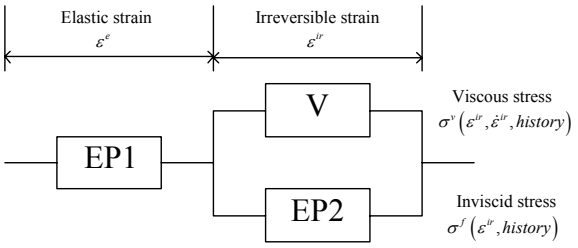

Figure 9. Non-linear three-component model.

5 SIMULATION

5.1 *Three-component model*

The observed load-strain-time behaviour of the PET yarn was simulated by the three-component model (**Fig. 9**), which was obtained by modifying the original version re-

placing the stress with the load. According to the model, the load V is given as follows in ML cases:

$$V = V^f\left(\varepsilon^{ir}\right) + V^v\left(\varepsilon^{ir}, \dot{\varepsilon}^{ir}\right) \quad (1)$$

where $V^f\left(\varepsilon^{ir}\right)$ is the inviscid load component that is a unique function of ε^{ir}. In the present study, the function $V^f\left(\varepsilon^{ir}\right)$, called the reference relation, was determined by fitting the following equation to the respective inferred $V^f - \varepsilon$ relation during ML at zero-strain rate that was extrapolated from the test result:

$$V^f = \sum_{i=1}^{10} a_i \cdot \left(\varepsilon^{ir}\right)^{i-1} \quad (2)$$

where a_i is the coefficient for term i. $V^v\left(\varepsilon^{ir}, \dot{\varepsilon}^{ir}\right)$ is the viscous load component that is a function of ε^{ir} and $\dot{\varepsilon}^{ir}$. Based on the fact presented in Fig. 8a, $V^v\left(\varepsilon^{ir}, \dot{\varepsilon}^{ir}\right)$, which corresponds to the load change ΔV upon a step change in $\dot{\varepsilon}^{ir}$, could be represented as follows:

$$V^v = V^f\left(\varepsilon^{ir}\right) \cdot g_v\left(\dot{\varepsilon}^{ir}\right) \quad (3)$$

Hence, Eq. 1 becomes:

$$V = V^f\left(\varepsilon^{ir}\right) \cdot \left\{1 + g_v\left(\dot{\varepsilon}^{ir}\right)\right\} \quad (4)$$

where $g_v\left(\dot{\varepsilon}^{ir}\right)$ is the viscosity function, for which the following function has been proposed for geomaterials (Di Benedetto et al., 2002; Tatsuoka et al., 2002):

$$g_v\left(\dot{\varepsilon}^{ir}\right) = \alpha \cdot \left[1 - \exp\left\{1 - \left(\left|\dot{\varepsilon}^{ir}\right| / \dot{\varepsilon}_r^{ir} + 1\right)^m\right\}\right] \quad (5)$$

where $\left|\dot{\varepsilon}^{ir}\right|$ is the absolute value of $\dot{\varepsilon}^{ir}$; α, m and $\dot{\varepsilon}_r^{ir}$ are the positive material constants. Note that the function $g_v\left(\dot{\varepsilon}^{ir}\right)$ is always positive whether during loading, unloading, reloading or so (i.e., irrespective of the sign of $\dot{\varepsilon}^{ir}$).

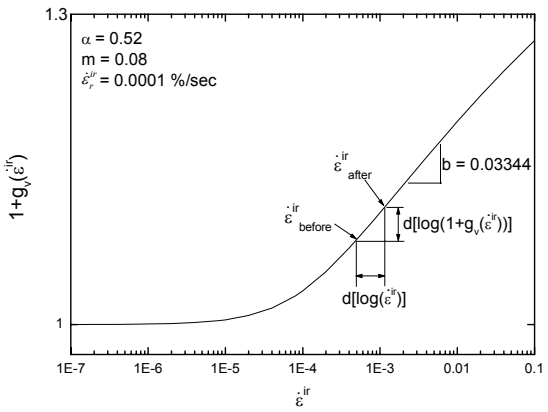

Figure 10. Viscosity function.

5.2 *Determination of model parameters*

Following Eq. 5, the parameters α and m were determined by trial and error in such a way that the linear part of the relationship between $\log\left(1 + g_v\left(\dot{\varepsilon}^{ir}\right)\right)$ and $\log(\dot{\varepsilon}^{ir})$ for a range of $\dot{\varepsilon}^{ir}$ encountered in the present test program has a slope b that is equal to $\beta / \ln(10)$, **Fig. 10**. This linear part cannot be extended towards zero as $\dot{\varepsilon}^{ir}$ decreases, but the value of $g_v\left(\dot{\varepsilon}^{ir}\right)$ should become zero as $\dot{\varepsilon}^{ir}$ becomes zero. The introduction of this non-linear relation is inevitable because V^v never becomes negative even when $\dot{\varepsilon}^{ir}$ becomes very small as long as $\dot{\varepsilon}^{ir}$ is positive.

The relation that $b = \beta / \ln(10)$ is obtained as follows. Suppose that $\dot{\varepsilon}^{ir}$ suddenly changes from $\dot{\varepsilon}^{ir}{}_{before}$ to $\dot{\varepsilon}^{ir}{}_{after}$ as depicted in Fig. 10. Then, the following equations are derived:

$$d\left[\log\left(1 + g_v\left(\dot{\varepsilon}^{ir}\right)\right)\right] = b \cdot \log\left(\dot{\varepsilon}^{ir}_{after} / \dot{\varepsilon}^{ir}_{before}\right) \quad (6a)$$

$$d\left[\ln\left(1 + g_v\left(\dot{\varepsilon}^{ir}\right)\right)\right] = b \cdot \ln\left(\dot{\varepsilon}^{ir}_{after} / \dot{\varepsilon}^{ir}_{before}\right) \quad (6b)$$

By substituting $V = V^f \cdot \{1 + g_v\left(\dot{\varepsilon}^{ir}\right)\}$ and $\Delta V^v = \Delta\left[V^f \cdot g_v\left(\dot{\varepsilon}^{ir}\right)\right] = V^f \cdot d\left[g_v\left(\dot{\varepsilon}^{ir}\right)\right]$ into the following linear relation with a slope β (Fig. 8b),

$$\Delta V / V = \Delta V^v / V = \beta \cdot \log\left(\dot{\varepsilon}^{ir}_{after} / \dot{\varepsilon}^{ir}_{before}\right) \quad (7a)$$

the following equation is derived:

$$\frac{V^f \cdot d\left[g_v\left(\dot{\varepsilon}^{ir}\right)\right]}{V^f \cdot \left[1 + g_v\left(\dot{\varepsilon}^{ir}\right)\right]} = d\left[\ln\left(1 + g_v\left(\dot{\varepsilon}^{ir}\right)\right)\right] = \beta \cdot \log\left(\dot{\varepsilon}^{ir}_{after} / \dot{\varepsilon}^{ir}_{before}\right) \quad (7b)$$

By comparing Eqs. 6b & 7b, the following equation that links the slopes b and β is obtained:

$$\beta = b \cdot \ln 10 \quad (8)$$

The determined values of α and m are 0.52 and 0.08, respectively, which provide the slope b in Fig. 10 equal to 0.03344, thus β = 0.077. This β value is very similar to the measured one, equal to 0.080. Finally, the value of $\dot{\varepsilon}^{ir}{}_r$, which does not change the slope b but shifts the curve laterally in Fig. 10, was determined so that the rate of creep strain and stress relaxation with different initial strain rates and at different load levels can be well simulated. As the value of $\dot{\varepsilon}^{ir}{}_r$ decreases, the viscous load component V^v increases. In the present study, $\dot{\varepsilon}^{ir}{}_r$ equal to 0.0001 %/sec was selected.

5.3 *Simulation of test results*

The simulated $V - \varepsilon$ relationships are presented in Figs. 4 & 5. It may be seen from these figures that the proposed model can simulate rather accurately the whole viscous aspects observed for a wide range of loading history, especially for: a) sudden increase/decrease in the load upon a stepwise change in the strain rate; b) different creep strains and rates for different load levels and different initial strain rates; and c) rate of load relaxation. It is to be noted that the same model parameters were used for all these tests. Some small discrepancy between the measured and simulated load-strain relations is due mostly to an inevitable scatter in the material properties among the different specimens.

6 CONCLUSIONS

The following conclusions can be derived from the results of experiment and simulation described in this paper:

1) The tensile load-strain behaviour during monotonic loading (ML) at a constant strain rate, upon stepwise changes in the strain rate, during creep loading and stress relaxation tests and the rupture strength of the tested PET yarn are significantly rate-dependent.
2) The stiffness of tensile load-strain relation upon the restart of loading after creep loading is very high, close to

the elastic behaviour, and subsequently it tends to re-join the original one that would be obtained from continuous ML test at the respective strain rate. This result indicates that the tensile load-strain behaviour is essentially a unique function of instantaneous irreversible strain rate.

3) The rupture strength is controlled uniquely by the strain rate at rupture, not affected by pre-rupture loading histories (with creep & relaxation tests). This implies that creep is not a degradation phenomenon and there is no reason to reduce the rupture strength of geosynthetic reinforcement measured at a certain strain rate by using a large creep reduction factor to obtain the long-term design strength unless the creep failure is likely to occur during a given design life time. Some corrections for a difference between the inferred strain rate at the failure of structure and the strain rate used in the material tests may be necessary.
4) The non-linear three-component model that was firstly developed for simulation of the time-dependent deformation characteristics of geomaterials is also relevant to geosynthetic reinforcements. A successful simulation of the test results obtained from the present study also validated the above.

7 ACKNOWLEDGEMENTS

The authors acknowledge Dipl. Ing. Gernot Mannsbart, Polyfelt GmbH, Austria, for providing us the test material. The financial support from the Ministry of Education, Culture and Sport, Japan, through the grant No. 13852011 is highly appreciated.

8 REFERENCE

Di Benedetto,H., Tatsuoka,F. and Ishihara,M., 2002: Time-dependant shear deformation characteristics of sand and their constitutive modelling, Soils and Foundations, Vol.42, No.2, pp.1-22.

Hirakawa,D, Uchimura,T., Shibata,Y. and Tatsuoka,F., 2002: Time-dependant deformation of geosynthetics and geosynthetic-reinforced soil structures, Proc. 7th International Conference on Geosynthetics, Nice, Vol.4, pp.1417-1430.

Hirakawa,D., Kongkitkul,W., Tatsuoka,F and Uchimura,T., 2003: Time-dependent stress-strain behaviour due to viscous properties of geosynthetic reinforcement, Geosynthetics International (accepted).

Kongkitkul,W, Hirakawa,D, Tatsuoka,F and Uchimura,T., 2003: Viscous deformation of geosynthetic reinforcement under cyclic loading conditions and its model simulation, Geosynthetics International (submitted).

Kongkitkul,W., Hirakawa,D. and Tatsuoka,F., 2002: Viscous deformation during cyclic loading of geosynthetics reinforcement, Proc. 7th International Conference on Geosynthetics, Nice, Vol.1, pp.129-132.

Tatsuoka,F., Ishihara,M., Di Benedetto,H. and Kuwano,R., 2002: Time-dependent shear deformation characteristics of geomaterials and their simulation", Soils and Foundations, Vol.42, No.2, pp.106-132.

Voskamp,W., Van Vliet,F. and Retzlaff,J., 2001: Residual strength of PET after more than 12 years creep loading, Proc. of the International Symposium on Earth Reinforcement (Ochiai et al., eds), Balkema, Vol.1, pp.165-170.